8-1993

Groundwater Velocity in an Unconfined Aquifer With Rectangular Areal Recharge

Vitaly A. Zlotnik
University of Nebraska-Lincoln, vzlotnik1@unl.edu

Glenn Ledder
University of Nebraska-Lincoln, gledder1@unl.edu

WATER RESOURCES RESEARCH, VOL. 29, NO. 8, PAGES 2827–2834, AUGUST 1993

Groundwater Velocity in an Unconfined Aquifer With Rectangular Areal Recharge

VITALY ZLOTNIK

Department of Geology, University of Nebraska at Lincoln

GLENN LEDDER

Department of Mathematics, University of Nebraska at Lincoln

Three-dimensional solutions for the hydraulic head and velocity components for transient groundwater flow in an unconfined compressible aquifer of finite thickness with a rectangular areal recharge source are analyzed using a linearized mathematical model. The solution generalizes Dagan's (1967) results, which were obtained for an idealized aquifer of infinite thickness, and Hantush's (1967) results, which were derived using the Dupuit assumptions. Hydraulic head and velocity components are estimated by asymptotic methods for large times, which are most appropriate for contaminant transport problems. Numerical analysis of the solution demonstrates spatial features of the velocity components in general and a transient effect of upward flow in particular, similar to that found for circular sources (Zlotnik and Ledder, 1992). Obtained formulas show that applicability of the Dupuit assumption for computation of velocity components in an unconfined aquifer is limited to a far-field zone given approximately by $|x| > 1.5X$, $|y| > 1.5Y$, where X and Y are the half width and half-length, respectively, of the contaminant source.

1. INTRODUCTION

Computation of groundwater velocities is an important component of modeling contaminant transport in the subsurface. However, our ability to predict transport in the saturated zone is often hampered by flow field complexities. Generally, the geometry of the flow field and the contaminant source in three-dimensional space can be represented by a superposition of point, line, and areal sources. Point and line sources were thoroughly studied in well hydraulics. A wide variety of analytical formulas for hydraulic head distributions are available for different well types and formations [*Streltsova*, 1988]. Such solutions usually have radial symmetry.

The shape of contamination sources often differs drastically from a circular form, however. Agrichemicals from spills, nonaqueous phase liquid from eroded pipelines, radionuclide losses from burial sites, etc., may enter an aquifer of finite thickness through rectangular areas having different aspect ratios. The corresponding flow field does not have axial symmetry. In this case the problem becomes essentially three-dimensional, and the solutions for infinite aquifer thickness or circular shape are not valid.

Solutions for the height of groundwater mounds under circular and rectangular sources of recharge were obtained by *Hantush* [1967] with Dupuit assumptions. These solutions completely ignore the vertical velocity component, and their applicability for horizontal velocity component calculations under and near the recharge area is questionable. Neglecting compressibility, *Dagan* [1967] obtained solutions for groundwater mound height and potential distribution for infinite strip, circular, and rectangular recharge areas in a thick unconfined aquifer and for infinite strip and circular recharge areas in unconfined aquifers of finite thickness. Formal three-dimensional solutions for mound height and potential distribution for circular and rectangular sources were obtained for a compressible aquifer of finite thickness by *Zlotnik* [1990], generalizing the solutions (for a circular source and an incompressible aquifer) of *Dagan* [1967]. However, no analysis of velocity components was given by any of these authors. Analysis of the three-dimensional flow under a circular source in an unconfined aquifer with arbitrary thickness was done first by *Zlotnik and Ledder* [1992]. It was established that the role of compressibility in recharge problems is unimportant for the practical range of parameters (unlike well problems [*Neuman*, 1974]). The problem considered here is the analysis of velocity in an unconfined aquifer with a rectangular area of recharge.

Generally, three-dimensional flow problems can be addressed by application of hydraulic head-based finite element or finite difference techniques. Then the velocity distribution is derived by various differentiation techniques. The accuracy of this procedure for each case study is difficult to determine. Another approach based on the derivation of a boundary value problem for velocity directly [*Zijl*, 1984] was applied for steady state flow in two dimensions [*Frind and Matanga*, 1985; *Zheng et al.*, 1988]. However, no realistic analytical solutions for velocity components were available for verification of numerical solutions of three-dimensional unsteady problems [*Herbert*, 1985].

This paper demonstrates the use of analytical formulas for unsteady three-dimensional hydraulic head and velocity components in an unconfined aquifer of finite thickness with a rectangular source of recharge, along with asymptotic formulas and some recommendations for simplified velocity calculations based on Dupuit assumptions. The spatial properties of the velocity distributions are described; of particular interest is the occurrence of a transient upward velocity component during the recharge process. The results have

Paper number 93WR00969.
0043-1397/93/93WR-00969$05.00

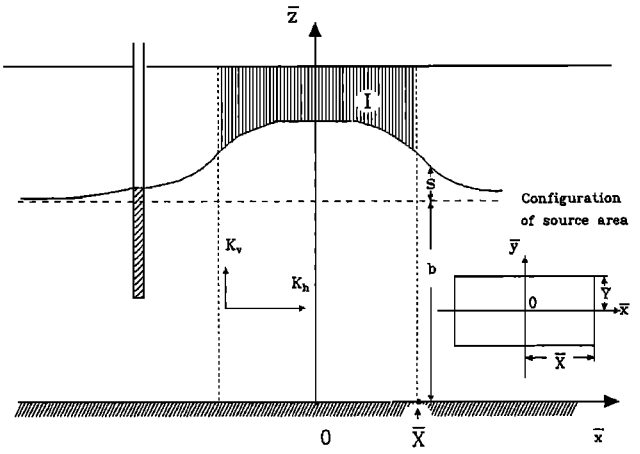

Fig. 1. Schematic diagram of groundwater recharge in an unconfined aquifer with finite thickness.

important qualitative and quantitative implications for the solution of three-dimensional problems of contaminant transport and the delineation of spatial capture zones with particle tracking techniques.

2. Problem Statement

We consider an unconfined aquifer of infinite lateral extent and finite thickness that rests on an impermeable horizontal layer. The aquifer material is uniform and anisotropic, with the principal conductivities being oriented parallel to the coordinate axes. The net specific recharge I at the water table is uniformly distributed over a rectangular area of half-length $\bar{X}$ and half width $\bar{Y}$ (Figure 1). The effects of the free surface and the compressibility of the aquifer material and water are included following *Neuman* [1974].

Under the assumption $I \ll K_v$ (following *Dagan* [1967]) the governing equations for the increase of hydraulic head for $-\infty < \bar{x}, \bar{y} < \infty$, $0 < \bar{z} < b$, $\bar{t} > 0$ may be linearized as follows:

$$K_h\left(\frac{\partial^2 \bar{s}}{\partial \bar{x}^2} + \frac{\partial^2 \bar{s}}{\partial \bar{y}^2}\right) + K_v \frac{\partial^2 \bar{s}}{\partial \bar{z}^2} = S_s \frac{\partial \bar{s}}{\partial \bar{t}} \tag{1}$$

$$\lim_{|\bar{x}|+|\bar{y}|\to\infty} \bar{s}(\bar{x}, \bar{y}, \bar{z}, \bar{t}) = 0; \qquad \frac{\partial \bar{s}}{\partial \bar{z}}(\bar{x}, \bar{y}, 0, \bar{t}) = 0 \tag{2}$$

$$K_v \frac{\partial \bar{s}}{\partial \bar{z}}(\bar{x}, \bar{y}, b, \bar{t}) + S_y \frac{\partial \bar{s}}{\partial \bar{t}}(\bar{x}, \bar{y}, b, \bar{t}) = \bar{I}(\bar{x}, \bar{y}, \bar{t}) \tag{3}$$

$$\bar{I}(\bar{x}, \bar{y}, \bar{t}) = IH(\bar{X} - |\bar{x}|)H(\bar{Y} - |\bar{y}|)H(\bar{t}); \tag{4}$$

$$H(x) = 0,\ x < 0 \quad H(x) = 1/2,\ x = 0 \quad H(x) = 1,\ x > 0$$

$$\bar{s}(\bar{x}, \bar{y}, \bar{z}, 0) = 0 \tag{5}$$

where $\bar{s}$ is the increase of hydraulic head over the initial value, $\bar{x}$, $\bar{y}$, $\bar{z}$ are the Cartesian dimensional coordinates, $\bar{t}$ is the dimensional time, $\bar{X}$ and $\bar{Y}$ are the half-length and half width of the rectangular source, b is the initial saturated thickness of an aquifer, K_h and K_v are the horizontal and vertical conductivities, S_s is the specific (elastic) storage, S_y is the specific yield, and I is the intensity of groundwater recharge (beginning at $\bar{t} = 0$) within the rectangular source.

3. Solution for the Hydraulic Head

The compressibility parameter $\sigma = S_s b/S_y$ is very small under most circumstances and has little effect for times of the order of the reference time

$$t_v = S_y b/K_v \tag{6}$$

[*Zlotnik and Ledder*, 1992]. For most aquifers, t_v is of the order of a few hours or less. Transport problems require a much larger time scale, so we may assume $\sigma = 0$ for practical determination of flow velocities. We define dimensionless variables by

$$z = \frac{\bar{z}}{b},\ x = \frac{\bar{x}}{b}\left(\frac{K_v}{K_h}\right)^{1/2},\ y = \frac{\bar{y}}{b}\left(\frac{K_v}{K_h}\right)^{1/2},\quad t = \frac{\bar{t}}{t_v} \tag{7}$$

$$s(x, y, z, t) = \frac{K_v}{Ib}\bar{s}[\bar{x}(x), \bar{y}(y), \bar{z}(z), \bar{t}(t)] \tag{8}$$

Because of the symmetry in the problem, we may consider the equivalent problem on the space $x > 0$, $y > 0$, $0 < z < 1$ with appropriate boundary conditions at $x = 0$, $y = 0$. In terms of the new variables, the problem takes the form

$$\frac{\partial^2 s}{\partial x^2} + \frac{\partial^2 s}{\partial y^2} + \frac{\partial^2 s}{\partial z^2} = 0 \tag{9}$$

$$s(\infty, y, z, t) = s(x, \infty, z, t) = 0 \tag{10}$$

$$\frac{\partial s}{\partial x}(0, y, z, t) = \frac{\partial s}{\partial y}(x, 0, z, t) = \frac{\partial s}{\partial z}(x, y, 0, t) = 0 \tag{11}$$

$$\frac{\partial s}{\partial z}(x, y, 1, t) + \frac{\partial s}{\partial t}(x, y, 1, t) = H(X - x)H(Y - y)H(t) \tag{12}$$

$$s(x, y, z, 0) = 0 \tag{13}$$

where

$$X = \frac{\bar{X}}{b}\left(\frac{K_v}{K_h}\right)^{1/2}, \qquad Y = \frac{\bar{Y}}{b}\left(\frac{K_v}{K_h}\right)^{1/2} \tag{14}$$

The problem (9)–(13) can be solved by applying the Laplace transform in time and the double Fourier cosine transform in the horizontal Cartesian coordinates. Derivations are given in the appendix. The solution is

$$s = \frac{4}{\pi^2}\int_0^\infty \int_0^\infty \Pi(a_1, a_2, x, y)\Phi(a, z, t)\frac{da_1\, da_2}{a_1 a_2} \tag{15}$$

where

$$\Pi(a_1, a_2, x, y) = \cos(a_1 x)\sin(a_1 X)\cos(a_2 y)\sin(a_2 Y) \tag{16}$$

$$\Phi(a, z, t) = (1 - e^{-ta\tanh a})\frac{\cosh az}{a \sinh a},\quad a = (a_1^2 + a_2^2)^{1/2} \tag{17}$$

The elevation of the water table above its initial position is approximately equal to the hydraulic head increase at the initial level of water table ($z = 1$) [*Dagan*, 1967].

4. SOLUTION FOR THE VELOCITY FIELD

Once the increase in hydraulic head has been determined, the explicit derivation of velocity components from (15) by differentiation is straightforward:

$$V_x = -\partial s/\partial x, \qquad V_y = -\partial s/\partial y, \qquad V_z = -\partial s/\partial z \tag{18}$$

and the structure of corresponding functions is similar to (15). The dimensional velocity field is then given by

$$\bar{V}_x = I(K_h/K_v)^{1/2}V_x, \quad \bar{V}_y = I(K_h/K_v)^{1/2}V_y, \quad \bar{V}_z = IV_z \tag{19}$$

For analysis and numerical computation, it is convenient to replace Cartesian integration variables a_1 and a_2 in (15) and (18) for velocity components with variables in polar coordinates ($a_1 = X^{-1}r\cos\theta$, $a_2 = X^{-1}r\sin\theta$):

$$V_x = \frac{4}{\pi^2}\int_0^\infty \left[1 - g\left(\frac{r}{X}, t\right)\right]\xi_H\left(\frac{r}{H}, z\right) \cdot \chi_H(r, \bar{x}, \bar{y}, \beta)\, dr \tag{20}$$

$$V_y = \frac{4}{\pi^2}\int_0^\infty \left[1 - g\left(\frac{r}{Y}, t\right)\right]\xi_H\left(\frac{r}{Y}, z\right) \cdot \chi_H(r, \bar{y}, \bar{x}, \beta^{-1})\, dr \tag{21}$$

$$V_z = -\frac{4}{\pi^2}\int_0^\infty \left[1 - g\left(\frac{r}{X}, t\right)\right]\xi_V\left(\frac{r}{X}, z\right) \cdot \chi_V(r, \bar{x}, \bar{y}, \beta)\, dr \tag{22}$$

where

$$\bar{x} = x/X, \qquad \bar{y} = y/Y, \qquad \beta = Y/X \tag{23}$$

$$g(a, t) = e^{-ta\tanh a},$$

$$\xi_H(a, z) = \cosh az/\sinh a, \tag{24}$$

$$\xi_V(a, z) = \sinh az/\sinh a$$

$$\chi_H(r, u, v, c) = \frac{1}{r}\int_0^{\pi/2} \frac{\sin(ur\cos\theta)W(r, v, c, \theta)}{\sin\theta}\, d\theta \tag{25}$$

$$\chi_V(r, u, v, c) = \frac{2}{r}\int_0^{\pi/2} \frac{\cos(ur\cos\theta)W(r, v, c, \theta)}{\sin 2\theta}\, d\theta \tag{26}$$

$$W(r, v, c, \theta) = \sin(r\cos\theta)\cos(cvr\sin\theta)\sin(cr\sin\theta) \tag{27}$$

Vertical velocity at $z = 1$ can be obtained directly from the boundary condition (12)

$$V_z|_{z=1} = -H(1 - \bar{x})H(1 - \bar{y}) + \frac{4}{\pi^2}\int_0^\infty g\left(\frac{r}{X}, t\right)\chi_V(r, \bar{x}, \bar{y}, \beta)\, dr \tag{28}$$

5. LONG-TIME ANALYSIS

Since the appropriate time scale for particle tracking is much larger than the time scale of velocity changes, the behavior of the velocity components as $t \gg 1$ is of particular interest.

Steady state velocity components $V_{x,\infty}$, $V_{y,\infty}$, $V_{z,\infty}$ are determined numerically from (20)–(22) by setting $g = 0$. Then the deviations of the velocity components V_x, V_y, V_z from their steady state values are given by

$$V_x - V_{x,\infty} = -4\pi^{-2}\int_0^\infty g(X^{-1}r, t)\xi_H(X^{-1}r, z) \cdot \chi_H(r, \bar{x}, \bar{y}, \beta)\, dr \tag{29}$$

$$V_y - V_{y,\infty} = -4\pi^{-2}\int_0^\infty g(Y^{-1}r, t)\xi_H(Y^{-1}r, z) \cdot \chi_H(r, \bar{y}, \bar{x}, \beta^{-1})\, dr \tag{30}$$

$$V_z - V_{z,\infty} = 4\pi^{-2}\int_0^\infty g(X^{-1}r, t)\xi_V(X^{-1}r, z) \cdot \chi_V(r, \bar{x}, \bar{y}, \beta)\, dr \tag{31}$$

The asymptotic behavior of these deviations for long times can be determined by applying Laplace's method for the asymptotic expansion of integrals with a large parameter [*Bender and Orszag*, 1978] to the general form

$$J(\bar{x}, \bar{y}, z, t) = \int_0^\infty g(\alpha^{-1}r, t)F(r, \bar{x}, \bar{y}, z)\, dr, \qquad t \gg 1 \tag{32}$$

where g is given by (24), α is a parameter, and the asymptotic behavior of F is given by

$$F \sim r^n\psi(\bar{x}, \bar{y}, z), \qquad r \to 0 \tag{33}$$

with the result

$$J \sim \frac{\Gamma(p)\alpha^{2p}}{2t^p}\psi(\bar{x}, \bar{y}, z), \qquad p = \frac{n+1}{2} \tag{34}$$

The function ψ and constants n and α for (33) are obtained from (29)–(31). Then from (34) we obtain long time approximations of the transient behavior of the velocity components as

$$V_x - V_{x,\infty} \sim -Ax/8\pi t, \qquad V_y - V_{y,\infty} \sim -Ay/8\pi t, \qquad V_z - V_{z,\infty} \sim Az/4\pi t \tag{35}$$

where $A = 4XY$ is the area of the recharge. Each of these approximations is valid when t is large enough to make the quantities on the right-hand sides of (32) small. The factors x and y which appear in the first two results indicate that the horizontal velocity components in the far field ($|x| > 1.5X$ or $|y| > 1.5Y$) approach their steady values slowly compared to points near the recharge area. Application of (32)–(34) to

$$\frac{\partial s}{\partial t}(x, y, 1, t) = \frac{4}{\pi^2}\int_0^\infty g\left(\frac{r}{X}, t\right)\chi_V(r, \bar{x}, \bar{y}, \beta)\, dr \tag{36}$$

yields the result

$$\frac{\partial s}{\partial t}(x, y, 1, t) \sim \frac{A}{4\pi t} \tag{37}$$

Integration of (37) with respect to time yields the long-time behavior of the groundwater mound:

$$s \sim \frac{A}{4\pi} \ln \frac{t}{t_0(x, y)} \tag{38}$$

where t_0 must be determined numerically.

The results (35) and (38) are independent of the aspect ratio β. The long-time deviation of the velocity components from the steady state and the long-time behavior of the hydraulic head are proportional to the source area, as previously determined for a circular source [*Zlotnik and Ledder*, 1992]. It thus appears likely that they are correct for a recharge area of any shape.

Under some circumstances it is useful to have a formula for the vertical average of the horizontal velocity components

$$\langle V_x \rangle_\infty = \int_0^1 V_{x,\infty}\, dz, \quad \langle V_y \rangle_\infty = \int_0^1 V_{y,\infty}\, dz$$

for points outside the recharge area. The steady state value of these average velocity components can be determined analytically from (15) by assigning $g = 0$ and using known definite integral formulas (3.725.3, 3.741.3, 3.947.2 [*Gradshtein and Ryzhik*, 1980]) for all combinations of $x < X$ or $x > X$ and $y < Y$ or $y > Y$. The results may be expressed in the form

$$\langle V_x \rangle_\infty = m_{xX} H(Y - y) - \pi^{-1} \cdot [U(x, X, Y - y) + U(x, X, Y + y)] \tag{39}$$

$$\langle V_y \rangle_\infty = m_{yY} H(X - x) - \pi^{-1} \cdot [U(y, Y, X - x) + U(y, Y, X + x)] \tag{40}$$

where $m_{AB} = \min\{A, B\}$ and

$$U(A, B, C) = \frac{A}{2} \tan^{-1}\left(\frac{2BC}{C^2 + A^2 - B^2}\right) + \frac{B}{2} \tan^{-1}\left(\frac{2AC}{C^2 + B^2 - A^2}\right) + \frac{C}{4} \ln \frac{C^2 + (A - B)^2}{C^2 + (A + B)^2} \tag{41}$$

6. Particle Tracking and Path Lines

Formulas for velocity components can be used for modeling of advective transport of contaminants in unconfined aquifers. One of the most common techniques of simulating advective contaminant transport is particle tracking. Corresponding Lagrange equations for single particle trajectory $x(t)$, $y(t)$, $z(t)$ are

$$\phi \frac{d\bar{x}}{d\bar{t}} = \bar{V}_x, \qquad \phi \frac{d\bar{y}}{d\bar{t}} = \bar{V}_y, \qquad \phi \frac{d\bar{z}}{d\bar{t}} = \bar{V}_z \tag{42}$$

where ϕ is porosity of the media. The dimensionless forms of these equations after using (7) and (19) are

$$dx/dt = \varepsilon V_x, \qquad dy/dt = \varepsilon V_y, \qquad dz/dt = \varepsilon V_z, \qquad \varepsilon = S_y I/\phi K_v \tag{43}$$

Changes in particle position are generally small for time period $t = O(1)$ (or $\bar{t}$ of order t_v), since ε is a small parameter due to the assumption $I \ll K_v$ of the linearized model. (For singularity zones, such as those near the edge of the recharge areas, such transitions can be significant.)

For particle tracking, another time scale and corresponding dimensionless time are more appropriate:

$$t_f = \phi b/I, \qquad t' = \bar{t}/t_f = \varepsilon t \tag{44}$$

The dimensionless forms of (42) in new variables are

$$\frac{dx}{dt'} = V_x\left(x, y, z, \frac{t'}{\varepsilon}\right), \quad \frac{dy}{dt'} = V_y\left(x, y, z, \frac{t'}{\varepsilon}\right), \quad \frac{dz}{dt'} = V_z\left(x, y, z, \frac{t'}{\varepsilon}\right) \tag{45}$$

Since t_f is much larger than t_v, velocity components approach the steady state by time $\bar{t} = O(t_f)$ according to (35). Generally, the transient components of the velocity can be ignored in flow calculations for $t = O(t_f)$; however, transient velocity components (which are of $O(\varepsilon)$) may be significant in regions where the steady state velocities are small. This last fact is important for transport computations. Most (if not all) known multidimensional analytical considerations of advective transport are based on the assumption of steady state flow, as predicted by (45), where t'/ε is large for $\bar{t} = O(t_f)$. As will be seen in a specific example, path lines based on steady state velocity calculations may be misleading.

7. Discussion of Results

It is worth noting the limitation of this approach. Velocity components were derived using *Dagan*'s [1967] first-order linearization, stemming from the condition $I \ll K_v$. Velocity is not defined in the space between the initial and the current water table, and extrapolation is the only way to obtain estimates of velocity in the domain. Application of next order theory becomes impractical owing to the complexity of the calculations. Thus the approach developed here is valid when the elevation of the water table is small compared with the initial saturated thickness of the aquifer.

Dagan [1967] found that first-order theory confirms *Hantush*'s [1967] results on water table elevations if the aquifer thickness is significantly less than the characteristic horizontal length of the studied shapes of the recharge source. For infinitely deep aquifers, *Dagan* [1967] derived compact closed formulas for water mound elevations and potential distribution with both aforementioned limitations. However, the most common practical case (when aquifer thickness is comparable with source size) is not covered by either *Dagan*'s [1967] or *Hantush*'s [1967] results (see also *Hunt* [1971] and *Singh* [1976]).

In our discussion we will focus on the velocity components, which have not been previously studied. Figures 2–6 illustrate the dimensionless velocity components for a

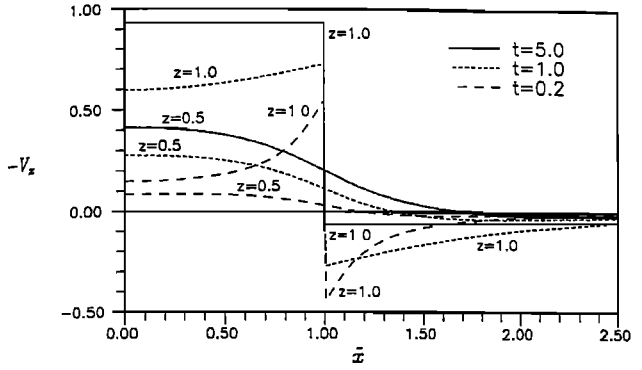

Fig. 2. Profiles of downward vertical velocity $-V_z$ versus x at various elevations z for different times, $y = 0$.

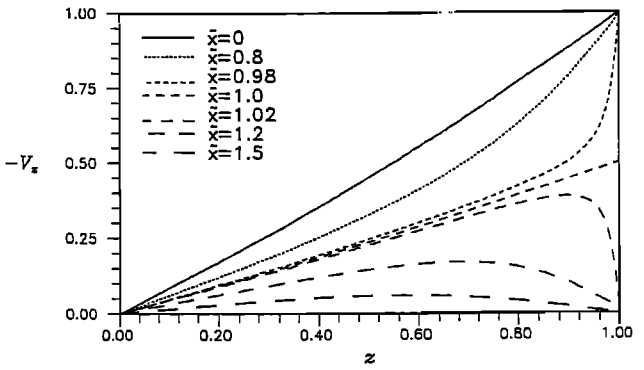

Fig. 3. Steady profiles of downward vertical velocity $-V_z$ versus elevation z at various x, $y = 0$.

square source with $X = 1$ (aquifer depth is $b = \bar{X}(K_v/K_h)^{1/2}$ by (14)). Other parameters do not affect the results for the dimensionless variables. Note that all graphs illustrate variation in one horizontal direction only, with all points corresponding to $y = 0$. FORTRAN programs that use International Mathematics and Statistics Libraries subroutines are available from the authors.

Vertical Velocity

Figure 2 illustrates the evolution of the transient solution of the downward vertical velocity to steady state for depths $z = 1$ and $z = 0.5$. The vertical velocity underneath the recharge area is always downward, but the magnitude depends on both z and x. For z near 1, the downward velocity is largest just inside the recharge area, but this dependence on x disappears as time increases. For intermediate depths, as illustrated by the curves for $z = 0.5$, the downward velocity is greater at the center of the recharge area than at the edge. Outside the recharge area there is a region where the vertical velocity is upward. For given t and $\bar{x}$, there is a critical depth $z_c(\bar{x}, t)$ with the property that the vertical velocity is upward for points above z_c and downward for points below z_c. As time increases, this critical z_c gradually increases; that is, only areas near the water table have upward flow. There are no points having an upward flow in the steady state. The existence of a region having an upward flow is a peculiarity of recharge problems with areal sources, since (12) gives $V_z = \partial s/\partial t > 0$ outside the recharge area at the surface $z = 1$, corresponding approximately to the water table in the linearized model.

The steady state downward velocity is further illustrated in Figure 3. Variations of downward velocity with x are gradual except near the top of the aquifer. The steady state vertical velocity at $z = 1$ is $-H(1 - |\bar{x}|)$, but the vertical velocity is a continuous function of z for any $\bar{x}$. Thus there are large variations of downward velocity with x near $z = 1$. At the center and the edge of the recharge area the vertical velocity is a linear function of z, but elsewhere, particularly near the edge of the source, linearity in z is not a good approximation. The assumption of linearity is valid for particular problems only, where the Dupuit assumption is a reasonable approximation [*Brainard and Gelhar*, 1992]. For points having $|x| > 1.5X$, the flow may be taken to be horizontal. The same is true for $|y| > 1.5Y$.

Horizontal Velocity

The approach to the steady state horizontal velocity for points having $y = 0$ is illustrated in Figure 4. The horizontal velocity is generally greatest at $x = X$, although the peak in the profile near the bottom of the aquifer shifts to a point outside the recharge area. At the top of the aquifer there is a singularity at the edge of the recharge area, where the horizontal velocity is infinite. This behavior is peculiar to recharge problems with areal sources having nonzero intensity at the source boundary. Note that the profiles for $z = 0.92$ and $z = 0$ converge at a point outside the recharge area, suggesting that variations of horizontal velocity with depth can be neglected at points sufficiently far away from the source.

The steady state horizontal velocity is further illustrated in Figures 5 and 6. Figure 5 shows variations with depth at points inside the recharge area, and Figure 6 gives the corresponding information for points outside the recharge area. Note that the horizontal velocity varies little with depth for $|x| > 1.5X$. In this region the vertically averaged horizontal velocity will be a good approximation to the pointwise horizontal velocity. Hence (34) can be used in place of (20). Similarly, (35) can replace (21) if $|y| > 1.5Y$.

The conditions $|x| > 1.5X$ and $|y| > 1.5Y$ give a practical range for the applicability of *Hantush* [1967] formulas and Dupuit assumptions for velocity calculations.

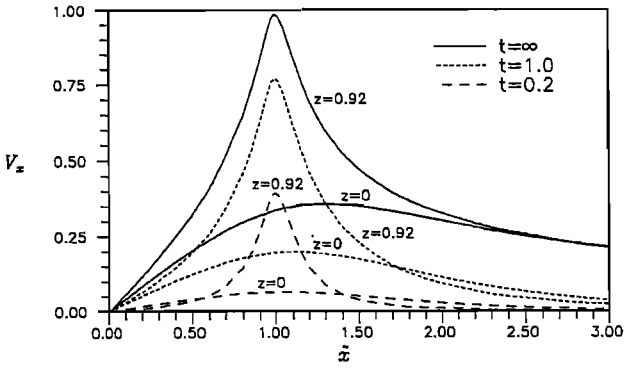

Fig. 4. Profiles of horizontal velocity V_x versus x at various elevations z for different times, $y = 0$.

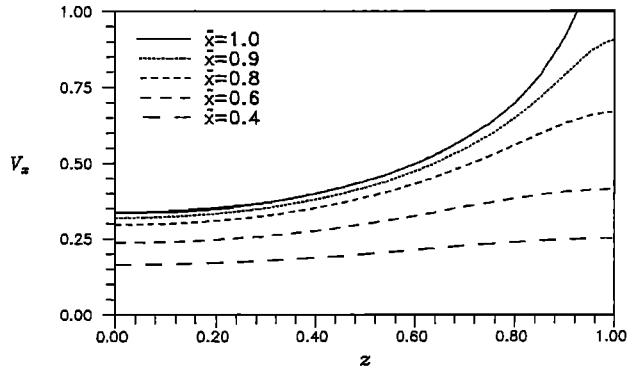

Fig. 5. Steady profiles of horizontal velocity V_x versus elevation z at various locations $x \leq X$, $y = 0$.

Path Lines

Path lines along the center- plane $y = 0$ are illustrated by the solid curves in Figure 7*a*, for a specific example ($I = 0.1$ m/d, $K_v = K_h = 10$ m/d, $S_y = 0.2$, $\theta = 0.25$, $b = \bar{X} = \bar{Y} = 20$ m). Also shown in Figure 7*a* are the positions of the front and the water table at $\bar{t} = 60$ days. The pathlines shown are for particles that begin at $z = 1$ at time $\bar{t} = 0$. Particles starting at later times would have slightly different pathlines. The position of the front above $z = 1$ has been extended to the water table by extrapolation.

Figure 7*b* shows path lines, front, and water table for the infinite strip $\bar{Y} = \infty$ corresponding to the parameters of Figure 7*a*. The calculations were made using the results of *Dagan* [1967]. The upward flow in the region $x > X$, $z > 0.8$ occurs because even for relatively large times, the $O(\varepsilon)$ (upward) transient component in the vertical velocity is larger than the steady state (downward) velocity. A comparison of Figures 7*a* and 7*b* shows the effect of lateral flow in the y direction. Progression of the front is noticeably retarded by lateral flow at the leading edge of the front, as is demonstrated by the shape of the front near the water table. The path lines are also affected by this decrease in flow in the x direction.

8. CONCLUSIONS

Three-dimensional formulas for the hydraulic head and velocity components in an unconfined aquifer with rectangular areal recharge were analyzed using asymptotic and numerical methods.

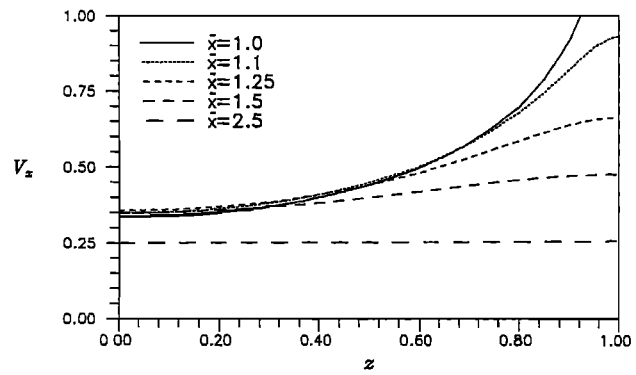

Fig. 6. Steady profiles of horizontal velocity V_x versus elevation z at various locations $x \geq X$, $y = 0$.

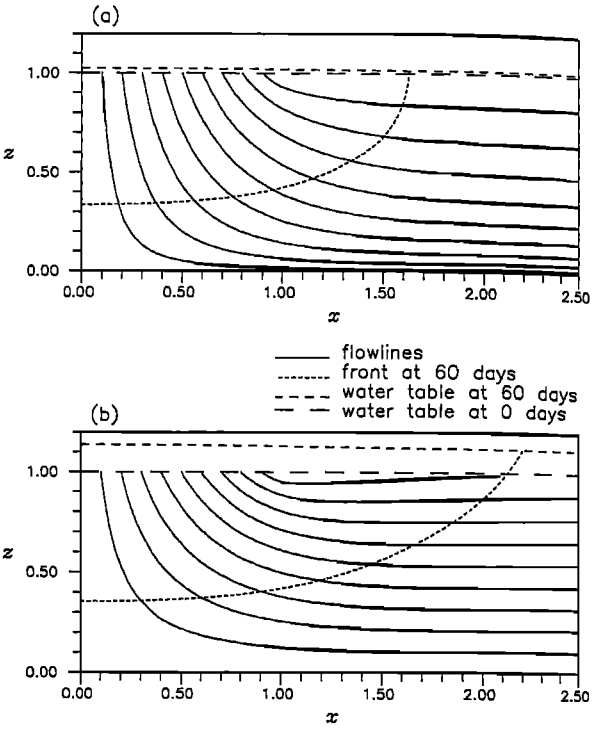

Fig. 7. Path lines on the $y = 0$ plane along with front and water table ($\bar{t} = 60$ days) for a specific case ($I = 0.1$ m/d, $K_v = K_h = 10$ m/d, $S_y = 0.2$, $\theta = 0.25$, $b = 20$ m) for (*a*) the square $\bar{X} = \bar{Y} = 20$ m and (*b*) the strip $\bar{X} = 20$ m, $\bar{Y} = \infty$.

The hydraulic head and mound elevation show logarithmic growth for large time, but velocity components approach a steady state. For times $\bar{t} > S_y b/K_v$, the deviations of velocity components from the steady state are proportional to At^{-1} and are independent of the shape of the areal source.

To summarize the principal features of the velocity field, the aquifer can be roughly divided into four concentric regions. From inside to outside, these are the central ($|x| < 0.5X$, $|y| < 0.5Y$), interior ($|x| < X$, $|y| < Y$, but outside the central region), exterior ($|x| < 1.5X$, $|y| < 1.5Y$, but outside the interior region), and far field ($|x| > 1.5X$ or $|y| > 1.5Y$).

In the central region the vertical velocity is largely independent of x and y and varies linearly with z. The horizontal velocity varies linearly with horizontal distance and increases slightly with z.

In the interior region the vertical and horizontal velocity components show large nonlinear variation with depth near the top of the aquifer. The horizontal velocity also shows a large nonlinear variation with position near the top, with a singularity at $z = 1$ for points at the edge of the source.

The distribution of the steady state velocity components in the exterior region mirrors that for the interior region, with large gradients near the top of the aquifer and small gradients in the middle and bottom. However, a transient hydrodynamic effect is observed in the exterior region, whereby the vertical velocity above some point on any vertical line is upward rather than downward. As time increases, the surface separating upward flow from downward flow rises,

approaching the water table (or $z \approx 1$) for $t \gg 1$. The upward transient flow is a direct result of the areal source geometry.

In the far field the vertical velocity is negligible and the horizontal velocity is approximately independent of depth, as suggested by the Dupuit assumption. In this region, simple formulas for the vertically averaged horizontal velocity may be used in place of the formulas for the pointwise horizontal velocity.

There are essential discrepancies between the steady state velocity distributions for Dupuit and three-dimensional flow, especially near the areal source. The obtained results can be used to refine the estimation of the three-dimensional spread of contaminants.

APPENDIX: DERIVATION OF THE SOLUTION

For any function $f(x, y, z, t)$ we define $\bar{f}(x, y, z, t)$ to be the Laplace transform [*Sneddon*, 1972]) of f:

$$\bar{f}(x, y, z, p) = \int_0^\infty e^{-pt} f(x, y, z, t)\, dt \qquad \text{(A1)}$$

$$f(x, y, z, t) = \frac{1}{2\pi i} \int_{\gamma - i\infty}^{\gamma + i\infty} e^{pt} \bar{f}(x, y, z, p)\, dp \qquad \text{(A2)}$$

For any function $\bar{f}(x, y, z, p)$ we define f^* to be the double Fourier cosine transform of $\bar{f}$ with respect to x and y:

$$f^*(a_1, a_2, z, p) = \int_0^\infty \int_0^\infty \bar{f}(x, y, z, p) \cos a_1 x \cos a_2 y\, dx\, dy \qquad \text{(A3)}$$

$$\bar{f}(x, y, z, p) = \frac{4}{\pi^2} \int_0^\infty \int_0^\infty f^*(a_1, a_2, z, p) \cos a_1 x \cdot \cos a_2 y\, da_1\, da_2 \qquad \text{(A4)}$$

Consecutively applying Laplace and Fourier cosine transforms to (9)–(12) yields the boundary value problem

$$\frac{\partial^2 s^*(a_1, a_2, z, p)}{\partial z^2} - a^2 s^*(a_1, a_2, z, p) = 0, \qquad \text{(A5)}$$

$$a^2 = a_1^2 + a_2^2$$

$$\frac{\partial s^*(a_1, a_2, 0, p)}{\partial z} = 0 \qquad \text{(A6)}$$

$$\frac{\partial s^*(a_1, a_2, 1, p)}{\partial z} + p s^*(a_1, a_2, 1, p) = \frac{\sin a_1 X \sin a_2 Y}{p a_1 a_2} \qquad \text{(A7)}$$

The solution of this boundary value problem is standard [*Neuman*, 1974; *Zlotnik and Ledder*, 1992]:

$$s^* = \frac{\sin a_1 X \sin a_2 Y}{p a_1 a_2} \frac{\cosh az}{a \sinh a + p \cosh a} \qquad \text{(A8)}$$

Inverting the Laplace transform first and using inverse Fourier transform (A4) yields the solution (15)–(17).

NOTATION

A	dimensionless area of rectangular source, equal to $4XY$.
b	initial saturated thickness of the aquifer.
H	unit step function.
I	net specific recharge at the water table.
K_h, K_v	horizontal and vertical hydraulic conductivity.
s, $\bar{s}$	dimensionless and dimensional hydraulic head increase.
S_s	specific (elastic) storage.
S_y	specific yield.
$\bar{t}$	dimensional time.
t	dimensionless time relative to t_v.
t'	dimensionless time relative to t_f.
t_f	time scale for advective transport.
t_v	time scale for velocity changes.
V_x, V_y	dimensionless horizontal velocity components.
$\langle V_x \rangle$, $\langle V_y \rangle$	vertically averaged horizontal velocities.
V_z	dimensionless (upward) vertical velocity.
x, y, $\bar{x}$, $\bar{y}$	dimensionless and dimensional horizontal coordinates.
X, Y, $\bar{X}$, $\bar{Y}$	dimensionless and dimensional half lengths of source.
$\bar{x}$, $\bar{y}$	ratio of horizontal coordinate to source half length.
z, $\bar{z}$	dimensionless and dimensional vertical coordinate.
β	aspect ratio, equal to Y/X.
σ	compressibility parameter.
ϕ	porosity.
ε	ratio of time scales (t_v/t_f).

Acknowledgment. This research was partially supported by the Water Center of the University of Nebraska at Lincoln. Development of software for IBM RISC 6000 systems was partially supported by IBM.

REFERENCES

Bender, C. M., and S. A. Orszag, *Advanced Mathematical Methods for Scientists and Engineers*, McGraw-Hill, New York, 1978.

Brainard, E. C., and L. W. Gelhar, Influence of vertical flow on ground-water transport, *Ground Water*, *29*(5), 693–701, 1992.

Dagan, G., Linearized solutins of free-surface groundwater flow with uniform recharge, *J. Geophys. Res.*, *72*(4), 1183–1193, 1967.

Frind, E. O., and G. B. Matanga, The dual formulation of flow and contaminant transport modeling, 1, Review of theory and accuracy aspects, *Water Resour. Res.*, *21*(2), 159–169, 1985.

Gradshtein, I. S., and I. M. Ryzhik, *Tables of Integrals, Series and Products*, Academic, San Diego, Calif., 1980.

Hantush, M. S., Growth and decay of groundwater-mounds in response to uniform percolation, *Water Resour. Res.*, *3*(2), 227–234, 1967.

Herbert, A. W., Analytical solutions to the three-dimensional radionuclide transport equation for computer code verification, *Appl. Math. Modell.*, *9*(3), 154–162, 1985.

Hunt, B. W., Vertical recharge of unconfined aquifers, *J. Hydraul. Div. Am. Soc. Civ. Eng.*, *97*(7), 1017–1030, 1971.

Neuman, S. P., Effect of partial penetration on flow in unconfined aquifers considering delayed gravity response, *Water Resour. Res.*, *10*(2), 303–312, 1974.

Singh, R., Prediction of mound geometry under recharge basins, *Water Resour. Res.*, *12*(4), 775–780, 1976.

Sneddon, I. H., *The Use of Integral Transforms*, McGraw-Hill, New York, 1972.

Streltsova, T. D., *Well Testing in Heterogeneous Formations*, John Wiley, New York, 1988.

Zheng, C., K. R. Bradbury, and M. P. Anderson, Role of interceptor ditches in limiting the spread of contaminants in ground water, *Ground Water*, *26*(6), 734–742, 1988.

Zijl, W., Finite-element methods based on a transport velocity representation for groundwater motion, *Water Resour. Res.*, *20*(1), 137–145, 1984.

Zlotnik, V., Three-dimensional groundwater velocity in unconfined aquifer under irrigation, in *Transport and Mass Exchange in Sand and Gravel Aquifers, Field and Modeling Studies, Proceedings of International Conference and Workshop, Ottawa, Canada*, vol. 2, edited by G. Moltyaner, pp. 628–647, Atomic Energy of Canada, Chalk River, Ont., 1990.

Zlotnik, V., and G. Ledder, Groundwater flow in a compressible unconfined aquifer with uniform circular recharge, *Water Resour. Res.*, *28*(6), 1619–1630, 1992.

G. Ledder, Department of Mathematics, University of Nebraska at Lincoln, Lincoln, NE 68588-0323.

V. Zlotnik, Department of Geology, University of Nebraska at Lincoln, Lincoln, NE 68588-0323.

(Received April 27, 1992;
revised March 22, 1993;
accepted April 2, 1993.)